THERAPEUTIC ULTRASOUND HEAT PROPAGATION IN A CYLINDRICAL FOUR-LAYER PHANTOM

D.P. Oliveira*, L. M. A. Areias*, W.C.A. Pereira*, M.A. von Krüger*

*Programa de Engenharia Biomédica – COPPE – UFRJ, Rio de Janeiro, Brasil
e-mail: *debora_poliveira@hotmail.com*

Abstract: Ultrasound (US) diathermy is widely used in the treatment of musculoskeletal diseases, and its therapeutic effect is achieved when temperatures reach 40-45 °C. For temperatures above 45 °C damages to the tissues can occur. The present work is an experimental (infrared camera) and simulated (COMSOL Multiphysics®) study of the temperature distribution in a multi-layer phantom irradiated by therapeutic ultrasound. Temperatures in therapeutic levels were achieved for irradiation period of 300s and intensity of 2 W·cm^{-2}. Although temperatures ≥ 45 ºC were obtained only in simulated models, a temperature elevation higher than 8ºC was registered, reaching for both models values ≥20ºC. The study promotes a better understanding of the thermal field generated from US diathermy.
Keywords: IR Image, Phantom, Ultrasound.

Introduction

The clinical use of US has diagnostic and therapeutic applicability. One of the main goals of therapeutic ultrasound contemplates the heating of biological tissue to generate physiological changes that minimize a pathological condition (US diathermy). In US diathermy to achieve physiological effects such as analgesia and reduction of muscle spasms it is necessary that the temperature in the area to be treated remains at 40-45 ºC for at least 5 minutes. Therefore, temperatures below 40 °C are ineffective, whereas temperatures above 45 ºC are undesirable, as they can cause protein denaturation and tissue injury [1].

Ultrasonic phantoms are test bodies that mimic the properties of biological tissues. The advantage of using phantoms is to obtain a standardized model with well-defined acoustic properties for the study of complex biological structures [2].

This work presents an experimental and simulated study of the thermal field in a cylindrical four-layer phantom of right middle-arm irradiated by therapeutic ultrasound.

Methodology

A. The Four-layer Phantom Structure

A cylindrical four-layer phantom was built with three layers corresponding respectively to soft tissues (fat, muscle and bone marrow), made by a mixture of graphite powder and agarose-based material. The layer corresponding to cortical bone was a commercial epoxy resin-based phantom (Sawbones®, Pacific Research Laboratories, Inc; Vashon, Washington, USA).

The mean values for density, acoustic and thermal properties of the four layers that compose the phantom are listed in Tables 1 and 2.

Table 1: Density and acoustic properties of the phantom

Layer	Density and Acoustic Properties		
	Density (kg·m^{-3})	c (m·s^{-1})	α (db·cm^{-1}- 1MHz)
Fat	1118.36	1585.62	0.34
Muscle	1154.31	1572.50	0.65
Cortical Bone	1700.59	2948.26	5.73-6.17
Bone Marrow	1118.36	1585.62	0.34

Table 2: Thermal properties of the phantom

Layer	Thermal Properties		
	Specific Heat (J·kg^{-1}·K^{-1})	Conductivity (W·m^{-1}·K^{-1})	Thermal Emissivity
Fat	4842.35	0.46	1
Muscle	3299.47	0.76	1
Cortical Bone	1256.34	0.47	0.96
Bone Marrow	4842.35	0.46	1

Anthropometric dimensions were assumed in the phantom [3-6]. The phantom is split along its height in halves of 50-mm that are put together during US irradiation. Figures 1 illustrates the dimensions and final aspect of the phantom.

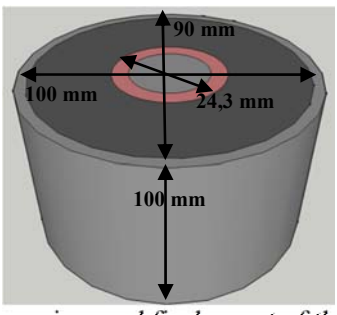

Figure 1: Dimensions and final aspect of the cylindrical four-layer phantom, with the two halves put together.

B. Experimental Procedures

A physiotherapy ultrasound equipment (Avatar III, KLD, Brazil), with approximately 2 years of use, was

applied to heat the phantoms. The irradiation protocol was: 1-MHz frequency; nominal intensities of 1.0, 1.5 and 2.0 W.cm^{-2}; irradiation duration 75, 150 and 300 seconds, with static transducer and continuous mode. A water based gel was used as a coupling medium between the phantoms and probe. The halves of the phantom were put together and the transducer was positioned on the lateral surface of the phantom on the radial direction and aligned with its central axis. Room temperature during the experiment was 21.0 ±1.8°C.

The images of the phantoms temperature distribution were obtained with an infrared camera (TM InfraCAM, Flir Systems, USA), plane focal matrix (FPA) of 120 x 120 pixels, accuracy ± 2.0 ºC and thermal sensitivity of 0.20 ºC. The temperature range was set between 25-45ºC. The camera was positioned on a tripod, which was 285 mm away from the phantom superficies (Figure 2). After US irradiation of the phantom, its two halves are split apart so that the infrared image can be made from the inside along of the layers. The time period for opening the phantom and capturing the thermal images after US irradiation was 3 seconds. The images were transferred to a computer for display and analysis. It was used the software Flir QuickPort 1.2 (FLIR Systems, 2008) to determine the spatial position and value of the maximum temperature (Tmax) and medium temperature (Tmed).

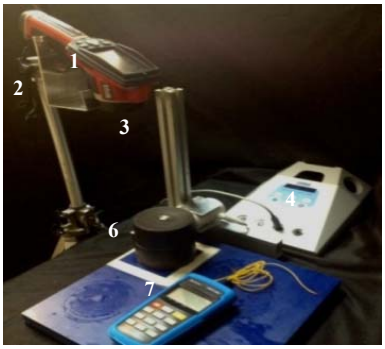

Figure 2: Experimental arrangement for US irradiation in the cylindrical four-layer phantom. In the image: 1) Infrared Camera; 2) Tripod; 3) Support for the US transducer; 4) Therapeutic US Equipment; 5) Transducer UST; 6) Cylindrical Four-layer Phantom and 7) Digital Thermometer.

C. Numerical Simulation

Numerical simulations of acoustic and heat propagations through the phantom were performed with the COMSOL Multiphysics® (version 4.3a, Los Angeles, CA, USA), a multiphysics modeling software that employs the finite element method. The diameter assumed for the ultrasound probe was 25 mm (value informed by the manufacturer of the therapeutic ultrasound equipment) and the type mesh employed was 0.3mm. The thickness of the layers, density and thermo-acoustic properties used in the numerical simulations were the same described in the first section and Tables I-II. The US irradiation parameters were the same of the experimental procedures and acoustic and thermal numerical simulations of US propagation were realized employing Equations 1-4.

$$\frac{\partial}{\partial r}\left[-\frac{r}{\rho_0}\left(\frac{\partial \rho}{\partial r}-q_r\right)\right]+r\frac{\partial}{\partial z}\left[-\frac{1}{\rho_0}\left(\frac{\partial \rho}{\partial z}-q_z\right)\right]-\left[\left(\frac{\omega}{c_0}\right)^2-\left(\frac{m}{r}\right)^2\right]\frac{r\rho}{\rho_0} \quad (1)$$

$$P = \sqrt{2\,Z\,I} \quad (2)$$

$$\rho C_p \frac{\partial T}{\partial t}+\rho C_p u_{trans}\cdot\nabla T+\nabla\cdot(-k\nabla T)=\rho_b C_b \omega_b (T_b-T)+Q_{met}+Q \quad (3)$$

$$Q = 2\alpha I = \alpha\rho c u_0^2 \quad (4)$$

In Equation (1) is expressed the wave equation for the proposed model that was simplified by (2) where *P* is the acoustic pressure, Z is acoustic impedance of the materials and *I* is the intensity of US bean. Equation 3 is Pennes´s bioheat equation that simplified by (4) where I is the intensity of US bean, α is the acoustic attenuation, ρ is the density, c is the US propagation velocity and u_0 is the particle velocity amplitude for each layer of the phantoms.

Results

The images of the temperature distribution from the inside of the phantom, obtained with the infrared camera, just after their halves are separated, are in Figures 3-5. As in the experimental models the images of the temperature distribution from numerical simulation are in Figures 6-8.

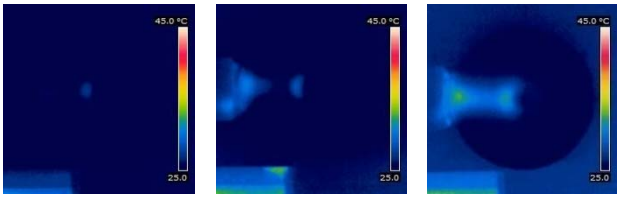

(A) **(B)** **(C)**

Figure 3: Experimental temperature distribution in the four-layer phantom produced by US irradiation at 1 MHz, after 75 seconds with nominal intensities: (A)1.0, (B)1.5 and (C)2.0 (W·cm^{-2}).

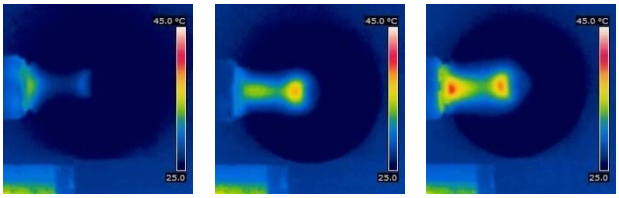

(A) **(B)** **(C)**

Figure 4: Temperature distribution in the four-layer phantom produced by ultrasonic irradiation at 1 MHz, after 150 seconds with nominal intensities: (A)1.0, (B) 1.5 and (C) 2.0 (W·cm^{-2}).

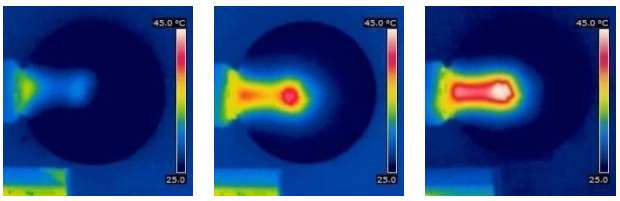

(A) (B) (C)

Figure 5: Temperature distribution in the four-layer phantom produced by ultrasonic irradiation at 1 MHz, after 300 seconds with nominal intensities: (A)1.0, (B) 1.5 and (C) 2.0 ($W \cdot cm^{-2}$).

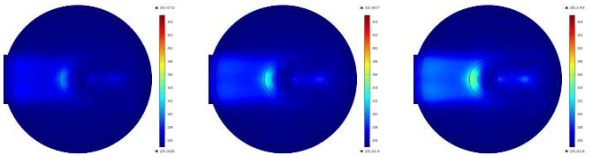

(A) (B) (C)

Figure 6: Simulated temperature distribution in the four-layer phantom produced by US irradiation at 1 MHz, after 75 seconds with nominal intensities: (A)1.0, (B) 1.5 and (C) 2.0 ($W \cdot cm^{-2}$).

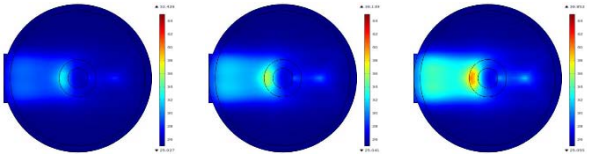

(A) (B) (C)

Figure 7: Simulated temperature distribution in the four-layer phantom produced by US irradiation at 1 MHz, after 150 seconds with nominal intensities: (A)1.0, (B) 1.5 and (C) 2.0 ($W \cdot cm^{-2}$).

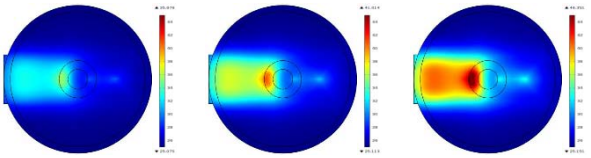

(A) (B) (C)

Figure 8: Simulated temperature distribution in the four-layer phantom produced by US irradiation at 1 MHz, after 300 seconds with nominal intensities: (A)1.0, (B) 1.5 and (C) 2.0 ($W \cdot cm^{-2}$).

A summary of respectively temperature distribution and temperature elevation in the phantom are represented in Tables 3-4 for experimental models and Tables 5-6 for simulated models. Where T_{med} are medium temperatures values, T_{max} are the maximum temperature values, TE_{med} are medium temperatures elevation values, and TE_{max} are the maximum temperature elevation values for each phantom layer. The expression of uncertainty measurement for T_{med} and TE_{med} were estimated in 2.49 °C, considering phantoms dimensions, distance from de IR camera and thermal emissivity. Influence of ambient temperature and relative humidity were also considered in uncertainty measurement.

Table 3: Temperature distribution (ºC) of the phantom for experimental model

Time (s)	Layer	Intensity ($W \cdot m^{-2}$) 1.0		1.5		2.0	
		T_{med}	T_{max}	T_{med}	T_{max}	T_{med}	T_{max}
75	Fat	24.00	26.18	26.68	30.46	29.18	33.36
	Muscle	23.60	26.06	24.60	29.34	27.90	32.72
	Cortical Bone	24.12	26.52	25.76	28.78	28.64	31.32
	Bone Marrow	23.22	25.36	23.84	26.60	26.56	29.68
150	Fat	29.60	31.86	29.44	34.76	32.04	38.54
	Muscle	25.54	30.08	28.48	35.14	30.44	37.94
	Cortical Bone	26.06	27.72	30.78	35.70	33.64	38.84
	Bone Marrow	24.66	26.38	27.36	31.20	29.46	35.34
300	Fat	31.94	37.14	34.48	39.48	36.60	44.54
	Muscle	28.18	34.22	32.70	41.68	33.08	43.22
	Cortical Bone	28.58	30.62	36.44	42.14	34.72	39.64
	Bone Marrow	26.76	29.34	32.60	38.62	31.68	35.62

Table 4: Temperature elevation (ºC) of the phantom for experimental model

Time (s)	Layer	Intensity ($W \cdot m^{-2}$) 1.0		1.5		2.0	
		TE_{med}	TE_{max}	TE_{med}	TE_{max}	TE_{med}	TE_{max}
75	Fat	3.00	5.18	5.68	9.46*	8.18*	12.36*
	Muscle	2.60	5.06	3.60	8.34*	6.90	11.72*
	Cortical Bone	3.12	5.52	4.76	7.78	7.64	10.32*
	Bone Marrow	2.22	4.36	2.84	5.60	5.56	8.68*
150	Fat	8.60*	10.86*	8.44*	13.76*	11.04*	17.54*
	Muscle	4.54	9.08*	7.48	14.14*	9.44*	16.94*
	Cortical Bone	5.06	6.72	9.78*	14.70*	12.64*	17.84*
	Bone Marrow	3.66	5.38	6.36	10.20*	8.46*	14.34*
300	Fat	10.94*	16.14*	13.48*	18.48*	15.60*	23.54*
	Muscle	7.18	13.22*	11.70*	20.68*	12.08*	22.22*
	Cortical Bone	7.58	9.62*	15.44*	21.14*	13.72*	18.64*
	Bone Marrow	5.76	8.34*	11.60*	17.62*	10.68*	14.62*

Table 5: Temperature distribution (ºC) of the phantom for simulated model

Time (s)	Layer	Intensity ($W \cdot m^{-2}$) 1.0		1.5		2.0	
		T_{med}	T_{max}	T_{med}	T_{max}	T_{med}	T_{max}
75	Fat	26.25	26.40	26.30	27.00	27.47	27.76
	Muscle	27.30	28.20	28.30	29.60	29.85	31.25
	Cortical Bone	28.90	30.07	30.70	32.43	32.65	35.68
	Bone Marrow	26.95	28.40	27.75	30.00	28.77	29.68
150	Fat	27.75	28.00	28.97	29.25	30.50	31.00
	Muscle	29.54	30.40	31.15	33.00	33.75	35.75
	Cortical Bone	31.10	32.61	34.04	36.14	37.18	41.01
	Bone Marrow	29.35	30.50	30.00	33.00	31.87	35.34
300	Fat	30.75	31.00	33.65	34.00	36.50	37.00
	Muscle	32.75	33.75	36.15	38.30	39.92	42.85
	Cortical Bone	34.34	35.14	39.00	39.85	43.73	46.35#
	Bone Marrow	30.95	33.40	33.85	37.70	37.00	42.00

Table 6: Temperature elevation (ºC) of the phantom for simulated model

Time (s)	Layer	Intensity (W·m^{-2})					
		1.0		1.5		2.0	
		TE_{med}	TE_{max}	TE_{med}	TE_{max}	TE_{med}	TE_{max}
75	Fat	1.25	1.40	1.30	2.00	2.47	2.76
	Muscle	2.30	3.20	3.30	4.60	4.85	6.25
	Cortical Bone	3.90	5.07	5.70	7.43	7.65	10.68*
	Bone Marrow	1.96	3.40	2.75	5.00	3.77	4.68
150	Fat	2.75	3.00	3.97	4.25	5.50	6.00
	Muscle	4.54	5.40	6.15	8.00	8.75*	10.75*
	Cortical Bone	6.10	7.61	9.04*	11.14*	12.18*	16.01*
	Bone Marrow	4.35	5.50	5.00	8.00	6.87	10.34*
300	Fat	5.75	6.00	8.65*	9.00*	11.50*	12.00*
	Muscle	7.75	8.75*	11.15*	13.30*	14.92*	17.85*
	Cortical Bone	9.34*	10.14*	14.00*	14.85*	18.73*	21.35*
	Bone Marrow	5.95	8.40*	8.85*	12.70*	12.00*	17.00*

Discussion

Due to its clinical relevance there are in the literature many studies that analyze the heat pattern and safety of US diathermy, employing invasive and non-invasive methods [7-9]. The present work presents, as a contribution, an experimental and simulated study of temperature distribution on a four-layer phantom (a standardized model) [2] using non-invasive method to access the thermal field generated by ultrasound (infrared camera and numerical simulation)

The temperature distribution was not uniform through the layers and hot spots can be detected in infrared images of the phantom either in experimental and simulated models (Figures 3-8). In simulated model hot spots can be observed beyond the area corresponding to the cortical bone mimics (Figures 3-8). This than can be attributed to limitation in the simulation software that consider phantom layers homogeneity and supposes that the layers of the phantom are in perfect match. For all conditions (intensity and time of US irradiation) the highest medium temperatures (T_{med}) were registered for the layers that mimic cortical bone (Table 3 and 4).

Experimental and simulated disagrees when fat mimics in simulated model registered the lowest values of temperature when compared to the other layers. In experimental model the layer corresponding to fat mimics registered high temperatures that can indicate poor complying or misalignment between the US probe and the phantom (Figures 3-5 and Table 3).

It is estimated that the thermal effects of the US occurs with elevation of biological tissue temperature to 40-45 ºC [1]. In experimental model therapeutic levels of temperatures were reached to the intensities of 1.5 and 2 W·cm^{-2} and exposition time of 300 seconds (Table 3), but only for temperature peak values (T_{max}). Therapeutic levels of temperatures were also reached in simulated model to the intensity of 2 W·cm^{-2} and exposition times of 300 seconds but for the layer that mimics cortical bone (Table 4). These hot spots can be attributed to the non-uniformity US thermal field (Figures 3-8).

Temperature elevation ≥ 4 ºC in biological tissues has been termed vigorous heating and is assumed to increase extensibility of collagen and decrease joint stiffness [10]. In this way, vigorous heating occurred in the intensity of 2 W·cm^{-2} independent of the US irradiation period; for the intensity ≥1.5 W·cm^{-2} and irradiation period ≥150 seconds; and for the intensity of 1 W·cm^{-2} and irradiation time of 300 seconds (Table IV and VI). The maximum temperature elevation (TE_{max}) registered was higher than 4 ºC for the all nominal intensities and irradiation periods in experimental models (Table IV). In simulated model TE_{max} ≥ 4ºC occurred only for intensity ≥ 1.5 W·cm^{-2} and irradiation period ≥150 seconds (Table 4 and 6).

Temperatures higher than 45 ºC and that can initiate protein denaturation in biological tissues were not registered in the experiments, but a temperature of 46.35ºC was registered for cortical bone mimic layer in simulated model (marked with "#" in Table 5). Such high temperature could be dangerous to the biological tissues if occurring in vivo. Temperature elevation higher than 8°C, considering temperature elevation linear and 37ºC as the baseline temperature of human body, could be potentially lesive to biological tissues, causing cellular damage and tissue lesion [1, 13]. Temperature elevation higher than 8°C was registered (marked with "*" in Table 4 and 6); with very high TE_{max} values (higher than 20°C) registered for 300s of US irradiation for the intensities of 1.5 and 2 W·cm^{-2} in both experimental and simulated models (Table 4 and 6).

A different temperature distribution is expected in biological tissues, with temperatures higher than that reached in experimental study, especially for fat and muscle, which, could be dangerous to those soft biological tissues. However, it is not possible to say with certainty if these high temperatures can occur in human biological tissues when using therapeutic US irradiation without considering other parameters like movement of US probe, the ability of human body in maintaining constant the corporal temperatures and the heat loss by the tissues perfusion.

Conclusion

This work has a potential impact on safety issues of therapeutic ultrasound application. Temperature therapeutic levels were achieved and although high temperatures (≥ 45 ºC) were not obtained, temperature elevations higher than 20ºC were registered in the phantom. If a temperature elevation as registered in the study, occured in biological tissues it would probably cause damage. A different heat pattern is expected in biological tissues, with higher temperatures especially for soft tissues. Complementary work should be done considering other US irradiating parameters and biological tissues metabolism to better elucidate this issue.

Acknowledgment

The authors would like to thank to CNPq, CAPES and FAPERJ for the financial support.

References

[1] Speed CA. Therapeutic ultrasound in soft tissue lesions. Rheumatology, Cambridge, v. 40, n. 12, p. 1331-1336, June 2001.

[2] Martin O, Culjat et al. A review of tissue substitutes for ultrasound imaging. Ultrasound in Medicine & Biology, v.36, n.6, pp.861–873, February 2010.

[3] Eston R, Evans R, Fu F. Estimation of body composition in Chinese and British men by ultrasonography assessment of segmental adipose tissue volume. Brazilian Journal of Sports Medicine, v.28, n.1, p. 9-13, 1994.

[4] Miyatani M, Kanehis H, Ito M, Kawakami Y, Fukunaga T. The accuracy of volume estimates using ultrasound muscle thickness measurements in different muscle groups. European Journal of Applied Physiology, v.91, p. 264-272, 2004.

[5] Qu X. Morphological effects of mechanical forces on the human humerus. Brazilian J. of Sports Medicine, v. 26, p.51-53, 1992.

[6] Pequini SM. Ergonomia aplicada ao design de produtos: um estudo de caso sobre o design de bicicletas. Tese (Doutorado) – Departamento de Tecnologia da Faculdade de Arquitetura e Urbanismo da Universidade de São Paulo, São Paulo, 2005.

[7] Oshikoya CA, Shultz SJ, Mistry D, Perrin DH, Arnold BL, Gansneder BM. Effect of Coupling Medium Temperature on Rate of Intramuscular Temperature Rise Using Continuous Utrasound. Journal of Athletic Training, v.35, n.4, p.417-421, 2000.

[8] Niikawa R, Sakuma S, Tanaka S, Tsuchiya T, Endoh N. Measurement of temperature rise in phantom using infrared imaging by varying pulse repetition frequency. In Proceedings of Symposium on Ultrasonic Electronics, v.32, p.407-408, 2011.

[9] Merrick MA, Bernard KD, Devor ST, Willians JM. Identical 3-MHz ultrasound treatments with different devices produce different intramuscular temperatures. Journal of Orthopaedic & Sports Physical Therapy, v.33, n.7, p.379-385, 2003.